*J. Fluid Mech.* (1984), *vol.* 149, *pp.* 339–353
*Printed in Great Britain*



# On a class of compressible laminar boundary-layer flows and the solution behaviour near separation

By ANTONIOS LIAKOPOULOS AND CHEN-CHI HSU
Department of Engineering Sciences, University of Florida, Gainesville, Florida 32611

(Received 16 December 1983 and in revised form 29 June 1984)

A class of compressible laminar boundary-layer flows subject to adverse pressure gradients of different magnitude is studied using a finite-element–differential method in which the assumed solutions are represented by classical cubic spline functions. The numerical integration process for the reduced initial-value problem has been carried out directly to at least one integration step upstream of the separation point, and very accurate numerical results have been obtained for a large number of integration steps extremely close to separation. The skin-friction and heat-transfer coefficients for nearly zero-heat-transfer, cooled-wall and heated-wall cases, computed under the assumption of constant Prandtl number $Pr = 1.0$ as well as $Pr = 0.72$, have clearly exhibited the same distinctive behaviour near separation. It is deduced that Buckmaster's series expansions for the solution near separation, derived on the assumptions of cooled wall and $Pr = 1.0$, are valid for all the cases considered. By matching the numerical results with Buckmaster's expansions, accurate distributions of skin friction and heat transfer have been obtained up to the separation point. Moreover, the importance of Prandtl number on the solution is evidenced from the numerical results presented.

## 1. Introduction

The development of a boundary layer under the action of a sharp adverse pressure gradient has been of special interest in compressible-flow analysis mainly because of its connection to shock-wave–boundary-layer interaction problems. It is well known that numerical methods for parabolic problems can provide accurate solutions of the governing equations for most of the boundary-layer flow region. However, close to separation the accuracy of the numerical results deteriorates to the extent that the true solution characteristics are lost and an interactive boundary-layer approach is necessary for a complete solution. Consequently, the accurate computation of the skin friction and heat transfer close to separation is a challenging problem. Moreover, an accurate solution near separation may provide valuable information for the solution of the Navier–Stokes equations involving a point of zero skin friction. Therefore a great deal of attention has been focused on resolving the true characteristics of the boundary-layer solutions near the separation point.

Two decades ago, Stewartson (1962) investigated the solution of a laminar compressible boundary layer near a point of zero skin friction. Following closely the approach introduced for the incompressible case (Goldstein 1948; Stewartson 1958), Stewartson concluded that a general compressible laminar boundary layer can develop a singularity at a point of zero skin friction only if the heat transfer at that point is zero. This conclusion was supported by the numerical results reported earlier by Poots (1960), and was not contradicted by those of Curle (1958). However, later

Merkin (1969) studied an incompressible boundary-layer flow over a vertical semi-infinite flat plate heated to a constant temperature in a uniform stream and reported the existence of a singularity at separation for the case of buoyancy forces opposing the development of the boundary layer. The numerical work of Merkin showed the need for a closer examination of Stewartson's expansion, since the convection problem solved by Merkin is mathematically analogous to that of a compressible boundary layer treated by Stewartson. In 1970 Buckmaster took a different approach in examining the compressible boundary-layer equations. Following Kaplun's (1967) analysis of the incompressible case, Buckmaster found for the cooled-wall case that a singularity can exist at a point of zero skin friction even if the heat transfer is not zero at that point.

A number of numerical investigations on the solution behaviour of compressible boundary-layer flows near separation have been reported after the publication of Buckmaster's work. Werle & Senechal (1973) considered linearly and quadratically retarded supersonic boundary-layer flows; their solutions offered evidence in support of Buckmaster's series expansions. Davies & Walker (1977) obtained numerical solutions for compressible flow past a circular cylinder and a linearly retarded flow and found that Buckmaster's expansions can be fitted to their numerical results not only for cooled walls but also for heated walls as well. More recently, Hunt & Wilks (1980) re-examined theoretically and numerically the behaviour of the laminar boundary-layer equations of mixed convection near a point of zero skin friction and demonstrated that Buckmaster's expansion is not an inherent feature of the coupling of the momentum and energy equations. They concluded that Stewartson's expansion is sufficient to describe the structure of the singularity at separation for the case of uniform heat flux at the wall.

The reported methods of solution for compressible boundary-layer flows can provide accurate results for most of the boundary-layer region; however, in the close vicinity of separation, they often fail to converge or give inaccurate results. For further positive assertion of Buckmaster's series expansion, highly accurate numerical results for the region extremely close to separation are needed. Hsu (1976) has developed a semidiscretization method for boundary-layer equations in which the transformed governing equations are reduced to a system of first-order nonlinear ordinary differential equations by a method of weighted residuals, and the assumed solutions at a streamwise station are represented by classical cubic spline functions. The resulting initial-value problem is integrated numerically by a predictor–corrector method. The method has been investigated in great detail on a number of different boundary-layer flow problems (e.g. Hsu & Chang 1982; Hsu & Liakopoulos 1982; Liakopoulos 1984), and has proved to be very effective. It can provide highly accurate results for nearly the entire boundary-layer region.

In the present work, a class of laminar compressible boundary-layer flows is studied using the developed semidiscretization method. Each boundary layer develops initially under zero pressure gradient and then separates under the action of an adverse pressure gradient which is proportional to a positive parameter $\lambda$. The problems solved include insulated-, cooled- and heated-wall cases for a wide range of values of the parameter $\lambda$. For all cases considered, the numerical integration process for the reduced initial-value problem has been carried out without any difficulty to at least one integration step upstream of the separation, and very accurate results have been obtained extremely close to separation. The computed skin-friction and heat-transfer coefficients near separation do exhibit the behaviour predicted by Buckmaster's expansion. Therefore, by coupling Buckmaster's series

solutions with the numerical results, we have obtained accurate distribution of skin friction and heat transfer for the entire boundary-layer region, including the heat transfer at the separation point. For the very sharp adverse-pressure-gradient cases the computed results are in good agreement with Curle's (1978) series solution, obtained under the assumptions $\lambda \to \infty$ and $Pr = 1$. The only exception is the value of the heat-transfer coefficient at separation, which we find relatively insensitive to wall-temperature conditions. Finally, a number of computations for fluids of Prandtl number different from unity have been performed. It has been found that the effect of Prandtl number is more pronounced for flows over cooled walls.

## 2. The governing equations

It is well known that the governing boundary-layer equations for steady, two-dimensional, laminar, compressible flow of perfect gases can be reduced to a form similar to those for incompressible flow by the Illingworth–Stewartson transformation if one assumes that the viscosity is linearly proportional to the temperature and that the Prandtl number $Pr$ is constant. Hence the transformed boundary-layer equations for the compressible flow are

$$\frac{\partial u}{\partial x}+\frac{\partial v}{\partial y}=0, \tag{1}$$

$$u\frac{\partial u}{\partial x}+v\frac{\partial u}{\partial y}=U_e\frac{\mathrm{d}U_e}{\mathrm{d}x}(1+S)+\nu_0\frac{\partial^2 U}{\partial y^2}, \tag{2}$$

$$u\frac{\partial S}{\partial x}+v\frac{\partial S}{\partial y}=\nu_0\left\{\frac{1}{Pr}\frac{\partial^2 S}{\partial y^2}+\alpha(x)\frac{\partial^2}{\partial y^2}\left[\left(\frac{u}{U_e}\right)^2\right]\right\}, \tag{3}$$

where

$$\alpha(x)\equiv\frac{(Pr-1)(\gamma-1)M_e^2(x)}{Pr[2+(\gamma-1)M_e^2(x)]}. \tag{4}$$

The subscript e denotes conditions at the outer edge of the boundary layer and $S$ is related to the temperature $T$ by

$$S\left(1+\frac{\gamma-1}{2}M_e^2\right)=\frac{T}{T_e}-1-\frac{\gamma-1}{2}M_e^2\left[1-\left(\frac{u}{U_e}\right)^2\right]. \tag{5}$$

Equation (5) clearly shows that $S$ becomes zero at the outer edge of the boundary layer and that at the wall we have

$$S_w=\frac{T_w}{T_0}-1, \quad T_0\equiv T_e[1+\tfrac{1}{2}(\gamma-1)M_e^2]. \tag{6}$$

Hence the associated boundary conditions considered are

$$u=0, \quad v=0, \quad S=S_w \quad \text{at} \quad y=0, \tag{7}$$

$$u\to U_e(x), \quad S\to 0 \quad \text{as} \quad y\to\infty. \tag{8}$$

As discussed by Hsu (1976), it is advantageous from the computational point of view to carry out a number of additional transformations. Since the growth rate of the boundary layer is not known beforehand, a transformation of Falkner–Skan type is introduced to suppress the variation in the boundary-layer thickness. The boundary conditions are made the same for all conceivable problems of the class. Moreover, a von Mises transformation is applied to reduce the number of dependent variables by one and to put the equations in the standard form of parabolic equations.

Following these transformations (given in the Appendix) the initial boundary-value problem to be solved, (1)–(8), becomes

$$\frac{\partial w}{\partial \xi} = \frac{w^{\frac{1}{2}}}{4}\left[\frac{1}{\eta^2}\frac{\partial^2 w}{\partial \eta^2} - \frac{1}{\eta^3}\frac{\partial w}{\partial \eta}\right] + \frac{\eta}{4}\frac{\partial w}{\partial \eta} + 2\left[(1-w) + \theta(1-\phi^{\frac{1}{2}})\right]\frac{\mathrm{d}\ln U}{\mathrm{d}\xi}, \tag{9}$$

$$\frac{\partial \phi}{\partial \xi} = \frac{w^{\frac{1}{2}}}{4Pr}\left[\frac{1}{\eta^2}\frac{\partial^2 \phi}{\partial \eta^2} - \frac{1}{\eta^3}\frac{\partial \phi}{\partial \eta} + \frac{1}{2\eta^2}\frac{\partial \ln(w/\phi)}{\partial \eta}\frac{\partial \phi}{\partial \eta}\right] + \frac{\eta}{4}\frac{\partial \phi}{\partial \eta} + 2(\phi^{\frac{1}{2}} - \phi)\frac{\mathrm{d}\ln\theta}{\mathrm{d}\xi} - \frac{\alpha(\xi)}{2\theta}\left(\frac{\phi}{w}\right)^{\frac{1}{2}}\left[\frac{w}{\eta^2}\frac{\partial^2 w}{\partial \eta^2} + \frac{1}{2\eta^2}\left(\frac{\partial w}{\partial \eta}\right)^2 - \frac{w}{\eta^3}\frac{\partial w}{\partial \eta}\right], \tag{10}$$

$$\alpha(\xi) \equiv \frac{(Pr-1)(\gamma-1)M^2(\xi)}{Pr[2+(\gamma-1)M^2(\xi)]}, \tag{11}$$

$$w(\xi,0) = 0, \quad \phi(\xi,0) = 0, \quad w(\xi,H) = 1, \quad \phi(\xi,H) = 1, \tag{12}$$

$$w(0^+,\eta) = w_0(\eta), \quad \phi(0^+,\eta) = \phi_0(\eta), \tag{13}$$

where $w(\xi,\eta)$ and $\phi(\xi,\eta)$ are the squares of the transformed velocity and temperature respectively, while $U(\xi)$, $\theta(\xi)$ and $M(\xi)$ are related to the given boundary conditions and reference parameters. The additional conditions, resulting from the physical boundary conditions and transformations, are

$$\frac{\partial w}{\partial \eta} = \frac{\partial \phi}{\partial \eta} = 0 \quad \text{at} \quad \eta = 0 \quad \text{and} \quad \eta = H. \tag{14}$$

We note that the conditions at infinity have been imposed at a sufficiently large finite distance $\eta = H$.

## 3. The numerical method

In the method of solution, the transformed solution profiles for $w(\xi,\eta)$ and $\phi(\xi,\eta)$ at a streamwise station $\xi$ are approximated by classical cubic spline functions. Suppose that the interval $0 \leqslant \eta \leqslant H$ is divided into $n$ elements with nodes at $0 = \eta_0 < \eta_1 < \ldots < \eta_n = H$. Denote the size of the $i$th element by $h_i = \eta_i - \eta_{i-1}$ for $i = 1, \ldots, n$ and the unknown functional values of the $j$th node by

$$w_j(\xi) = w(\xi,\eta_j), \quad \phi_j(\xi) = \phi(\xi,\eta_j). \tag{15}$$

The assumed solutions for $w(\xi,\eta)$ and $\phi(\xi,\eta)$ can be written (Hsu 1980) as

$$w(\xi,\eta) = \sum_{j=0}^{n} N_j(\eta)\, w_j(\xi), \tag{16}$$

$$\phi(\xi,\eta) = \sum_{j=0}^{n} N_j(\eta)\, \phi_j(\xi), \tag{17}$$

where

$$N_j(\eta) = \sum_{i=1}^{n} \delta_i\, a_{ij}(z), \quad \eta = z + \eta_{i-1}, \tag{18}$$

$a_{ij}$ are known polynomials of degree 3 or less in $z$, and

$$\delta_i = \begin{cases} 1 & \text{when} \quad \eta_{i-1} \leqslant \eta < \eta_i, \\ 0 & \text{otherwise.} \end{cases} \tag{19}$$

For the application of the method of weighted residuals, we have chosen the following set of weight functions for both (9) and (10):

$$\gamma_k(\eta) = \begin{cases} 1 & \text{when} \quad \eta_{k-1} \leqslant \eta < \eta_{k+1}, \\ 0 & \text{otherwise} \end{cases}, \quad k = 1, 2, \ldots, n-1. \tag{20}$$

Accordingly, we obtain the following system of equations:

$$\int_0^{h_k} \frac{\partial \bar{w}_k}{\partial \xi} \mathrm{d}z + \int_0^{h_{k+1}} \frac{\partial \bar{w}_{k+1}}{\partial \xi} \mathrm{d}z = \int_0^{h_k} R_w \, \mathrm{d}z + \int_0^{h_{k+1}} R_w \, \mathrm{d}z, \tag{21}$$

$$\int_0^{h_k} \frac{\partial \bar{\phi}_k}{\partial \xi} \mathrm{d}z + \int_0^{h_{k+1}} \frac{\partial \bar{\phi}_{k+1}}{\partial \xi} \mathrm{d}z = \int_0^{h_k} R_\phi \, \mathrm{d}z + \int_0^{h_{k+1}} R_\phi \, \mathrm{d}z, \tag{22}$$

where $\bar{w}_j$ and $\bar{\phi}_j$ are the cubic polynomials approximating $w(\xi, \eta)$ and $\phi(\xi, \eta)$ in the $j$th element, and $R_w$, $R_\phi$ represent the right-hand sides of (9) and (10) respectively. Equations (21) and (22) can be written in the matrix form

$$\frac{\mathrm{d}\boldsymbol{w}}{\mathrm{d}\xi} = \boldsymbol{A}^{-1}\boldsymbol{r}_1(\xi), \quad \frac{\mathrm{d}\boldsymbol{\phi}}{\mathrm{d}\xi} = \boldsymbol{A}^{-1}\boldsymbol{r}_2(\xi), \tag{23}$$

where $\boldsymbol{A}$ is an $n-1$ by $n-1$ non-singular constant matrix, which depends only upon the discretization in the $\eta$-direction. The $k$th elements of $\boldsymbol{r}_1$ and $\boldsymbol{r}_2$ are given by the right-hand sides of (21) and (22); they are accurately and efficiently evaluated with a Gauss–Legendre quadrature formula. The unknown $n-1$ dimensional vectors $\boldsymbol{w}$ and $\boldsymbol{\phi}$ are defined as

$$\boldsymbol{w}^{\mathrm{T}} \equiv [w_1(\xi), \ldots, w_{n-1}(\xi)], \quad \boldsymbol{\phi}^{\mathrm{T}} \equiv [\phi_1(\xi), \ldots, \phi_{n-1}(\xi)]. \tag{24}$$

The reduced initial-value problem (23) and (13) is solved with a predictor–corrector method based on the backward-difference formulas for stiff ordinary differential equations (Gear 1969). In this method the integration step size is automatically controlled by preassigned local error tolerance parameters. All computations were performed on an IBM 3081D computer in double-precision arithmetic.

## 4. Numerical results

For the numerical solution of the boundary-layer flow problem (1)–(8), we have assumed that the wall temperature is constant, i.e. $S_w$ = constant, and that the pressure distribution is uniform when $x \leqslant x_0$ but has a prescribed adverse gradient when $x > x_0$. Accordingly, the external velocity in (2) and (8) is specified by the following:

$$U_e(x) = U_0 = \text{const} \quad \text{when} \quad x \leqslant x_0, \tag{25}$$

$$U_e \frac{\mathrm{d}U_e}{\mathrm{d}x} = -\lambda \frac{U_0^2}{x_0(1+S_w)} \quad \text{when} \quad x > x_0, \tag{26}$$

where $\lambda$ is a positive constant. This class of problems, under the assumptions that $\lambda$ is large and $Pr = 1.0$, has been solved by Curle (1978) with a technique of matched asymptotic expansions. He found that the skin friction $Q_1$, the heat transfer $Q_2$ and the separation point $\zeta_s$ can be represented for large $\lambda$ and $x > x_0$ by the series

$$Q_1 \equiv \frac{2\nu_0 x}{U_0^3}\left(\frac{\partial u}{\partial y}\right)^2_{y=0} = F_0(\zeta) + \sigma_w \lambda^{-1} F_1(\zeta) + \sigma_w^2 \lambda^{-2} F_2(\zeta) + \ldots, \tag{27}$$

$$Q_2 \equiv -\left(\frac{2\nu_0 x}{U_0}\right)^{\frac{1}{2}} \frac{(\partial T/\partial y)_{y=0}}{T_w - T_0} = G_0(\zeta) + \sigma_w \lambda^{-1} G_1(\zeta) + \ldots, \tag{28}$$

$$\zeta_s = 0.09766 + 0.00403\,\sigma_w \lambda^{-1} + 0.00035\,\sigma_w^2 \lambda^{-2} + \ldots, \tag{29}$$

where $$\zeta = \lambda\left(\frac{x}{x_0} - 1\right)^{\frac{1}{3}}, \quad \sigma_w = \frac{S_w}{1 + S_w}.$$

For the transformed boundary-layer flow problem (9)–(13) the forcing functions in the governing equations take the forms

$$\theta(\xi) = S_w, \tag{30}$$

$$U(\xi) = \begin{cases} A^{\frac{1}{2}} \equiv [1 + \frac{1}{2}(\gamma - 1) M_\infty^2]^{\frac{1}{2}} & \text{when} \quad \xi \leqslant \xi_0 \equiv \ln\left(\dfrac{A^{\frac{1}{2}}}{\epsilon}\right), \\ A^{\frac{1}{2}} B^{\frac{1}{3}} \equiv A^{\frac{1}{2}}\left[1 + \dfrac{3\lambda}{1 + S_w}(1 - A^{-\frac{1}{2}} \epsilon\, e^{\xi})\right]^{\frac{1}{3}} & \text{when} \quad \xi > \xi_0, \end{cases} \tag{31}$$

$$\alpha(\xi) = \frac{(Pr - 1)(A - 1) U^2(\xi)}{Pr[A + (A - 1) U^2(\xi)]}, \tag{32}$$

where $\epsilon$ is a constant introduced to replace the zero integration limit in the Falkner–Skan transformation. The value $\epsilon = 10^{-6}$ has been used in the calculations. Moreover, the skin friction and heat transfer for $\xi > \xi_0$ become

$$Q_1 = \frac{U^4(\xi)[1 + (1 + S_w)(1 - B^2_3)/2\lambda]}{8\epsilon\, e^{\xi} A^{\frac{3}{2}}} \left(\frac{\partial^2 w}{\partial \eta^2}\right)^2_{\eta=0}, \tag{33}$$

$$Q_2 = \frac{U(\xi)[1 + (1 + S_w)(1 - B^2_3)/2\lambda]^{\frac{1}{2}}}{(8\epsilon\, e^{\xi})^{\frac{1}{2}} A^{\frac{1}{4}}} \left(\frac{\partial^2 w}{\partial \eta^2} \frac{\partial^2 \phi}{\partial \eta^2}\right)^{\frac{1}{2}}_{\eta=0}. \tag{34}$$

To assure the accuracy of the numerical solutions, a number of numerical experiments have been conducted. It was found that $H = 5.21$ is sufficiently large for imposing the outer boundary conditions. Solutions computed with larger values of $H$ were identical within the accuracy of the discretization used. An adaptive 36-element discretization model with element size distribution $h_i$ = /0.001, 0.0015, 0.0025, 0.005, 2*0.01, 2*0.02, 2*0.03, 2*0.04, 2*0.05, 2*0.1, 2*0.15, 2*0.2, 16*0.25/ has proved to give very accurate results. To assess the accuracy achieved, further runs were made using a refined discretization model having first-element size $h_1 = 0.0005$. In all cases, the absolute value of the differences in the computed skin-friction coefficient $Q_1$, as well as the heat-transfer coefficient $Q_2$, were less than $10^{-5}$ in the zero-pressure-gradient region and less than $10^{-4}$ in the adverse-pressure-gradient region of the boundary layer.

The first group of problems solved is the nearly zero-heat-transfer case with $Pr = 1.0$. To clarify the loosely defined condition 'large $\lambda$' assumed in the series solution, we have selected four different values of $\lambda$ and $S_w = 10^{-6}$. The computed separation points are given in table 1 in terms of Curle's coordinate $\zeta = \lambda(x/x_0 - 1)^{\frac{1}{3}}$. The computed skin friction $Q_1$ and heat transfer $Q_2$ are given in figures 1 and 2 respectively. It should be noted that the value of $Q_2$ at the separation point $\zeta_s$ is predicted from Buckmaster's series as discussed in §5. It is apparent that the separation point $\zeta_s$ does not vary appreciably when $\lambda$ is greater than or equal to one; furthermore, $\zeta_s = 0.0973$ agrees with the series solution (29) to the accuracy of the numerical solution. Similarly, the distributions of $Q_1$ and $Q_2$ for $\lambda = 1$ and $\lambda = 5$ agree with those obtained from (27) and (28). However, the agreement starts to deteriorate

| $\lambda$ | 5.00 | 1.00 | 0.20 | 0.02 |
|---|---|---|---|---|
| $\sigma_w \lambda^{-1}$ | $2 \times 10^{-7}$ | $10^{-6}$ | $5 \times 10^{-6}$ | $5 \times 10^{-5}$ |
| $\zeta_s$ | 0.09732 | 0.09734 | 0.09233 | 0.03343 |

TABLE 1. Computed separation points for various values of $\sigma_w \lambda^{-1}$; nearly zero heat transfer, $Pr = 1.0$

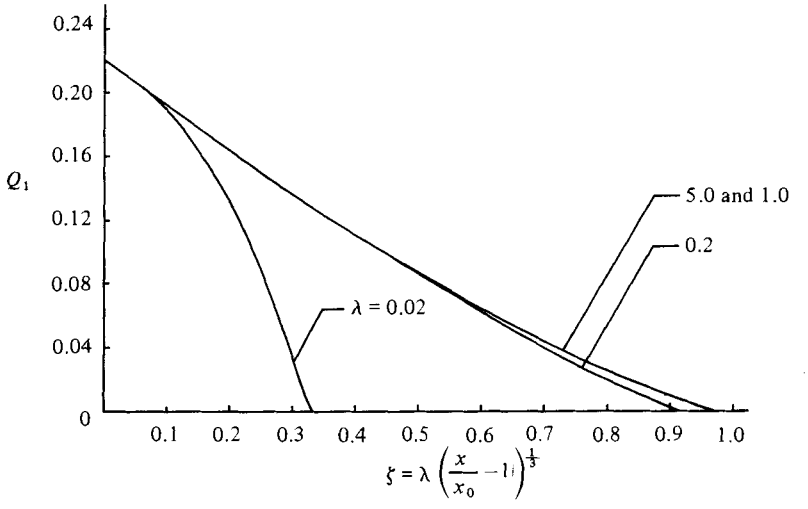


FIGURE 1. The skin-friction coefficient $Q_1$ for different values of $\lambda$ with $S_w = 10^{-6}$ and $Pr = 1.0$.

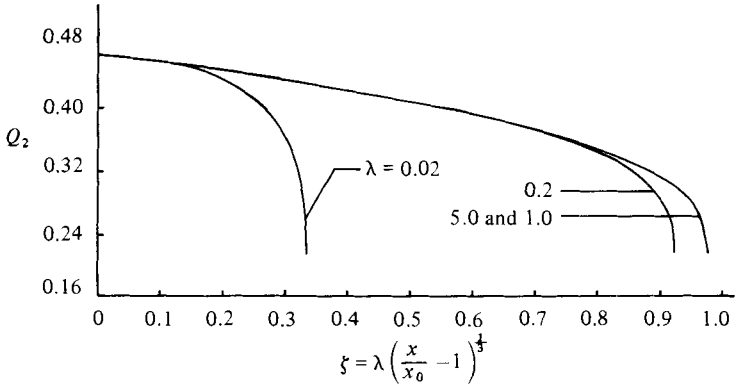


FIGURE 2. The heat-transfer coefficient $Q_2$ for different values of $\lambda$ with $S_w = 10^{-6}$ and $Pr = 1.0$.

as the value of $\lambda$ is decreased from one; in fact, the series (27)–(29) cannot be used for the case $\lambda = 0.02$, even though $|\sigma_w \lambda^{-1}| \ll 1$.

The numerical solutions obtained for the nearly zero-heat-transfer case imply that the loosely defined condition 'large $\lambda$' for (27)–(29) can be interpreted as $\lambda \geqslant 1$. In order to confirm further the conclusion on 'large $\lambda$', we have solved three additional problems with $\lambda = 1.0$ and $Pr = 1.0$: one with heated wall ($S_w > 0$) and two with cooled walls ($S_w < 0$). As shown in table 2, the computed separation points do agree with the series solution (29) to the third decimal place. Also, the computed skin-friction distribution agrees with the three-term series solution (27) at least to the third decimal place. Parenthetically, we remark that the published table for $F_0(\zeta)$ and $F_1(\zeta)$

| $S_w$ | $\sigma_w \lambda^{-1}$ | $\zeta_s$(computed) | $\zeta_s$((29)) |
|---|---|---|---|
| 1.0 | $\frac{1}{2}$ | 0.0995 | 0.0997 |
| $-\frac{1}{3}$ | $-\frac{1}{2}$ | 0.0954 | 0.0957 |
| $-\frac{1}{2}$ | $-1$ | 0.0936 | 0.0939 |

TABLE 2. Comparison of computed separation points with those predicted by (29), $Pr = 1.0$

and $F_2(\zeta)$ (Curle 1978) indicates that the magnitude of the third term is of order of $10^{-4}$. For the heat-transfer coefficient $Q_2$, the published table for $G_0(\zeta)$ and $G_1(\zeta)$ shows that the magnitude of the second term in (28) is of order of $10^{-2}$ for most of the region, except at the separation point, where it is of order of $10^{-1}$; hence we can expect the truncation error of the two-term series (28) to be as large as $10^{-1}$ in the vicinity of the separation. The comparison of the computed $Q_2$ with the results of the two-term series (28) shows that the difference increases to about 5% as $\zeta$ increases to $0.9\zeta_s$; moreover, the series solution gives $Q_2 = 0.08298$ at $\zeta_s$ for the heated-wall problem, while Buckmaster's series solution predicts $Q_2 = 0.218$ at separation. It is clear that the series for $Q_2$ converges rather slowly in the vicinity of the separation point.

The assumption of Prandtl number equal to unity is often made in order to simplify the governing energy equation (3) or (10); however, it is important to investigate the effect of Prandtl number on the skin-friction and heat-transfer coefficients. The inclusion of the viscous-dissipation term in the energy equation has little effect upon the accuracy and efficiency of the solution method. One heated-wall problem ($S_w = 1.0$ and $\sigma_w \lambda^{-1} = 0.5$) and one cooled-wall problem ($S_w = -0.5$ and $\sigma_w \lambda^{-1} = -1.0$) have been solved under the assumptions $Pr = 0.72$ and $M_\infty = 0.5$; the separation points computed are $\zeta_s = 0.0993$ and $\zeta_s = 0.0939$ respectively. The computed skin-friction coefficient $Q_1$ and heat-transfer coefficient $Q_2$, along with those for $Pr = 1.0$, are given in table 3. It is clear that the effect of Prandtl number on the separation point as well as the skin friction is rather nugatory; however, as expected, the effect of Prandtl number on the heat transfer is significant.

## 5. The behaviour of solutions close to separation

Numerical methods for parabolic problems can provide accurate solutions for most of the boundary-layer flow region; however, close to separation the accuracy of the numerical results often deteriorates to the extent that the correct characteristics of the solution are lost. The breakdown of numerical methods and the well-known loss of convergence of series solutions near separation suggest the existence of a singularity there. The structure of the singularity is well understood in the incompressible-flow case (e.g. Goldstein 1948; Stewartson 1958). However, the assumptions of the corresponding theory for compressible flow is still under investigation, and further numerical evidence is needed to support the analytical results (Hunt & Wilks 1980).

Following Kaplun's (1967) analysis of the incompressible case, Buckmaster (1970) has treated the compressible boundary-layer problem (1)–(8) for cooled walls ($S_w < 0$) with $Pr = 1.0$ and obtained series expansions for the solution near separation. His results for predicting skin friction and heat transfer may be written in the form

$$D_1(z) \equiv zf''(z,0) = z^2\left[2\alpha_0 \ln z + 2\alpha_1 + 2\alpha_2 \ln|\ln z| + 2\alpha_3 \frac{\ln|\ln z|}{\ln z} + \ldots\right], \tag{35}$$

Heated-wall case ($S_w = 1.0$, $\lambda = 1.0$)

| $\xi = \lambda\left(\frac{x}{x_0}-1\right)^{\frac{1}{3}}$ | $Q_1$ | | $Q_2$ | |
|---|---|---|---|---|
| | $Pr = 0.72$ | $Pr = 1.0$ | $Pr = 0.72$ | $Pr = 1.0$ |
| 0.000000 | 0.22052 | 0.22052 | 0.42111 | 0.49690 |
| 0.009977 | 0.19181 | 0.19171 | 0.41232 | 0.45969 |
| 0.019954 | 0.16417 | 0.16421 | 0.40312 | 0.44871 |
| 0.029930 | 0.13771 | 0.13787 | 0.39332 | 0.43706 |
| 0.039907 | 0.11264 | 0.11287 | 0.38265 | 0.42457 |
| 0.049884 | 0.08914 | 0.08930 | 0.37080 | 0.41098 |
| 0.059861 | 0.06700 | 0.06721 | 0.35768 | 0.39558 |
| 0.069838 | 0.04653 | 0.04681 | 0.34246 | 0.37782 |
| 0.079814 | 0.02830 | 0.02832 | 0.32380 | 0.35620 |
| 0.089791 | 0.01189 | 0.01217 | 0.29810 | 0.32650 |

Cooled-wall case ($S_w = -0.5$, $\lambda = 1.0$)

| $\zeta = \lambda\left(\frac{x}{x_0}-1\right)^{\frac{1}{3}}$ | $Q_1$ | | $Q_2$ | |
|---|---|---|---|---|
| | $Pr = 0.72$ | $Pr = 1.0$ | $Pr = 0.72$ | $Pr = 1.0$ |
| 0.000000 | 0.22052 | 0.22052 | 0.41201 | 0.46960 |
| 0.009395 | 0.19330 | 0.19329 | 0.40381 | 0.45978 |
| 0.018789 | 0.16670 | 0.16665 | 0.39529 | 0.44969 |
| 0.028184 | 0.14105 | 0.14094 | 0.38589 | 0.43823 |
| 0.037578 | 0.11626 | 0.11607 | 0.37575 | 0.42613 |
| 0.046973 | 0.09282 | 0.09255 | 0.36425 | 0.41234 |
| 0.056368 | 0.07046 | 0.07010 | 0.35138 | 0.39673 |
| 0.065762 | 0.04949 | 0.04905 | 0.33638 | 0.37861 |
| 0.075157 | 0.03030 | 0.02978 | 0.31786 | 0.35619 |
| 0.084551 | 0.01333 | 0.01278 | 0.29232 | 0.32499 |

TABLE 3. Skin-friction and heat-transfer coefficient distributions for $Pr = 1.0$ and $Pr = 0.72$

$$D_2(z) \equiv z^{-1}g'(z,0) = B_1 - zB_1 g_2'(0)\left[2\alpha_0 \ln z + 2\alpha_1 + 2\alpha_2 \ln|\ln z| + 2\alpha_3 \frac{\ln|\ln z|}{\ln z} + \ldots\right], \tag{36}$$

in which $f$ denotes a non-dimensional stream function and $g$ a dimensionless temperature function. The dimensionless distance $z$ measured from the separation point $x_s$ is defined as

$$z = \left(\frac{x_s - x}{l_s}\right)^{\frac{1}{4}}, \quad \frac{1}{l_s} \equiv -\left[\frac{1}{U_e}\frac{dU_e}{dx}(1+S_w)\right]_{x=x_s}, \tag{37}$$

in which the subscript s refers to conditions at the separation point. Moreover, Buckmaster showed that

$$\alpha_0 = \frac{-2\pi^{\frac{1}{2}}(-\frac{1}{4})!\,B_1}{64(\frac{1}{4}!)^3}, \quad \alpha_2 = (1-2\ln 2)\,\alpha_0,$$

$$\alpha_3 = \frac{-64(\frac{1}{4}!)^3\,\alpha_2^2}{2\pi^{\frac{1}{2}}(-\frac{1}{4})!\,B_1}, \quad g_2'(0) = \frac{-2^{\frac{1}{4}}\pi^{\frac{3}{2}}}{8(\frac{1}{4}!)^3},$$

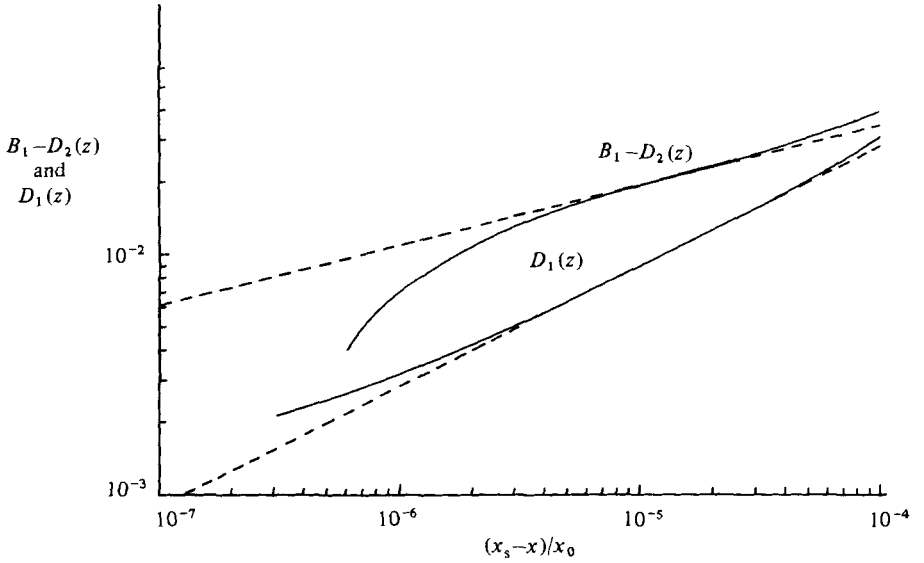


FIGURE 3. The distributions of $D_1(z)$ and $D_2(z)$ near separation for a heated-wall case, $\lambda = 1.0$, $S_w = 1.0$ and $Pr = 1.0$: ——, numerical results; – – –, Buckmaster's expansions with $\alpha_1 = 1.42$ and $B_1 = -0.109$.

while $\alpha_1$ and $B_1$ are two unknown constants to be determined. In terms of the transformed problem (9)–(13), we have

$$D_1(z) = \frac{1}{2}\left[\frac{U_0}{\lambda U_e(x_s) A^{\frac{3}{2}}}\right]^{\frac{1}{2}} \frac{U^2(\xi)}{(8\epsilon e^{\xi})^{\frac{1}{2}}}\left(\frac{\partial^2 w}{\partial \eta^2}\right)_{\eta=0}, \tag{38}$$

$$D_2(z) = \frac{-S_w}{1+S_w}\left[\frac{U_e(x_s)}{\lambda U_0 A^{\frac{1}{2}}}\right]^{\frac{1}{2}} \frac{U(\xi)}{(8\epsilon e^{\xi})^{\frac{1}{2}}}\left(\frac{\partial^2 w}{\partial \eta^2}\frac{\partial^2 \phi}{\partial \eta^2}\right)^{\frac{1}{2}}_{\eta=0}, \tag{39}$$

$$z = \left(\frac{1+S_w}{2}\right)^{\frac{1}{4}}\left[\left(\frac{B(\xi)}{B(\xi_s)}\right)^{\frac{2}{3}} - 1\right]^{\frac{1}{4}}, \tag{40}$$

in which the constant $A$ and the function $B(\xi)$ are defined in (31).

For the numerical method employed in this study the streamwise integration process can be carried out without any difficulty to at least one integration step upstream of the separation point. The computed $D_1(z)$ and $D_2(z)$ close to separation for a heated-wall case are presented in figure 3. Similar results are obtained in the cooled-wall case and the nearly zero-heat-transfer case. As expected, the accuracy of the computed skin friction starts to deteriorate somewhat in the region extremely close to separation, while the accuracy of $D_2(z)$ is drastically reduced. The loss of accuracy could have been recovered to some extent by using a more refined discretization model and a more stringent accuracy requirement in the integration process. It should be pointed out, however, that an accurate heat transfer at separation cannot be computed directly from (34) or (39), since the value of $\partial^2 w/\partial \eta^2$ at $\eta = 0$ approaches zero as $\xi$ approaches the separation point. Hence a special measure is required to predict the heat-transfer coefficient at separation.

The numerical results obtained for all the cases considered do exhibit the behaviour of the solution near separation predicted by Buckmaster's series solutions (35) and (36); that is, $D_1(z)$ is proportional to $(x_s - x)^{\frac{1}{2}}$ and $D_2(z)$ is proportional to $(x_s - x)^{\frac{1}{4}}$. In

| $\lambda$ | $S_w$ | $\sigma_w \lambda^{-1}$ | $\alpha_1$ | $B_1$ | $Q_2$ at separation |
|---|---|---|---|---|---|
| 5.0 | $10^{-6}$ | $2 \times 10^{-7}$ | 3.36 | $-0.097 \times 10^{-6}$ | 0.217 |
| 1.0 | $10^{-6}$ | $1 \times 10^{-6}$ | 1.43 | $-0.216 \times 10^{-6}$ | 0.216 |
| 0.2 | $10^{-6}$ | $5 \times 10^{-6}$ | 0.676 | $-0.455 \times 10^{-6}$ | 0.216 |
| 0.02 | $10^{-6}$ | $5 \times 10^{-5}$ | 0.523 | $-0.609 \times 10^{-6}$ | 0.216 |
| 1.0 | $-\frac{1}{3}$ | $-\frac{1}{2}$ | 1.46 | 0.107 | 0.216 |
| 1.0 | $-\frac{1}{2}$ | $-1.0$ | 1.49 | 0.211 | 0.216 |
| 1.0 | 1.0 | $\frac{1}{2}$ | 1.42 | $-0.109$ | 0.218 |

TABLE 4. Values of $\alpha_1$, $B_1$ and $Q_2$ at separation; $Pr = 1.0$

| $\frac{x}{x_0}$ | $10\zeta$ | $D_1(z)$, (38) | $D_1(z)$, (35) | $D_2(z)$, (39) | $D_2(z)$, (36) |
|---|---|---|---|---|---|
| 1.00070000 | 0.88791 | 0.04615 | 0.03846 | 0.1567 | 0.1472 |
| 1.00080002 | 0.92839 | 0.02684 | 0.02443 | 0.1436 | 0.1390 |
| — | — | — | — | — | — |
| 1.00085531 | 0.94924 | 0.01054 | 0.01045 | 0.1289 | 0.1280 |
| 1.00085631 | 0.94961 | 0.01008 | 0.01002 | 0.1284 | 0.1276 |
| 1.00085731 | 0.94998 | 0.00959 | 0.00956 | 0.1279 | 0.1271 |
| 1.00085801 | 0.95024 | 0.00925 | 0.00923 | 0.1274 | 0.1267 |
| 1.00085904 | 0.95061 | 0.00873 | 0.00873 | 0.1268 | 0.1262 |
| 1.00086033 | 0.95109 | 0.00802 | 0.00804 | 0.1259 | 0.1254 |
| 1.00086105 | 0.95136 | 0.00760 | 0.00763 | 0.1254 | 0.1250 |
| 1.00086214 | 0.95175 | 0.00693 | 0.00697 | 0.1245 | 0.1242 |
| 1.00086339 | 0.95222 | 0.00608 | 0.00612 | 0.1232 | 0.1231 |
| 1.00086435 | 0.95257 | 0.00535 | 0.00537 | 0.1221 | 0.1221 |
| 1.00086528 | 0.95291 | 0.00454 | 0.00453 | 0.1206 | 0.1208 |
| 1.0086628 | 0.95328 | 0.00350 | 0.00341 | 0.1189 | 0.1190 |

TABLE 5. Comparison of computed solution near separation point with that predicted by (35) and (36); $Pr = 1.0$

order to obtain accurate distributions of skin friction and heat transfer to the separation point we have used the truncated Buckmaster's series solutions given in (35) and (36). The two unknown constants involved, $\alpha_1$ and $B_1$, can be determined from a set of $D_1(z)$ and $D_2(z)$ computed from (38) and (39) at a station $z \ll 1$. For each of the flow cases considered we have determined $\alpha_1$ and $B_1$ at a number of streamwise stations. The variation of calculated $\alpha_1$ and $B_1$ is negligibly small for the accurate data very close to separation. The determined $\alpha_1$ and $B_1$ for the flow problems considered with the assumption of Prandtl number $Pr = 1.0$ are given in table 4. It is interesting to note that the wall temperature has little effect upon the value of $\alpha_1$ for the flow problems with pressure-gradient parameter $\lambda = 1.0$. The distributions of $D_1(z)$ and $D_2(z)$ computed from the truncated series (35) and (36) with the determined constants $\alpha_1$ and $B_1$ agree with the numerical solutions for an appreciable region of the boundary layer very close to separation. The results of a heated-wall case ($\lambda = 1.0$ and $S_w = 1.0$) are presented in figure 3. To demonstrate further the degree of agreement the comparison for the case $\lambda = 1$, $S_w = -\frac{1}{3}$ is presented in table 5.

The heat-transfer coefficient $Q_2$ defined in (28) can be related to $D_2(z)$ defined in

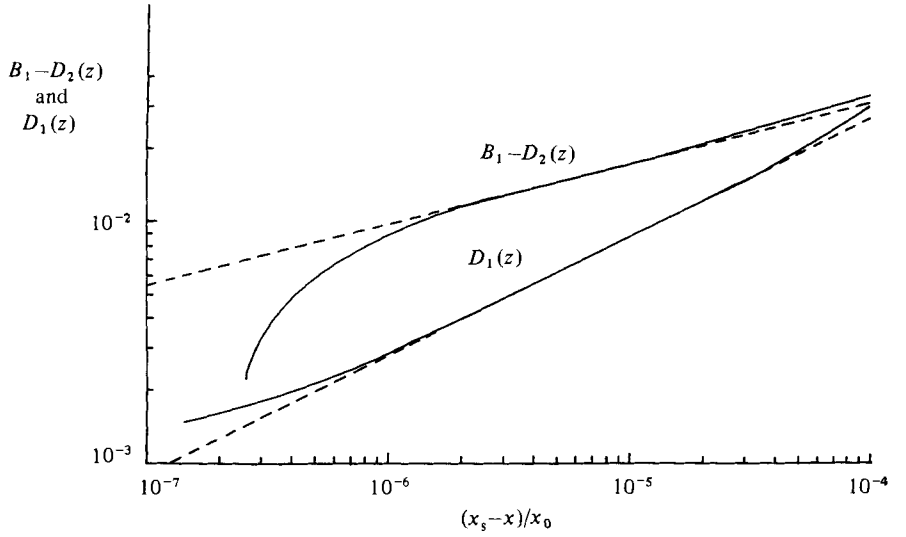


FIGURE 4. The distributions of $D_1(z)$ and $D_2(z)$ near separation for a heated-wall case ($\lambda = 1.0$ and $S_w = 1.0$) with Prandtl number = 0.72: ——, numerical results; – – –, Buckmaster's expansions with $\alpha_1 = 1.40$ and $B_1 = -0.102$.

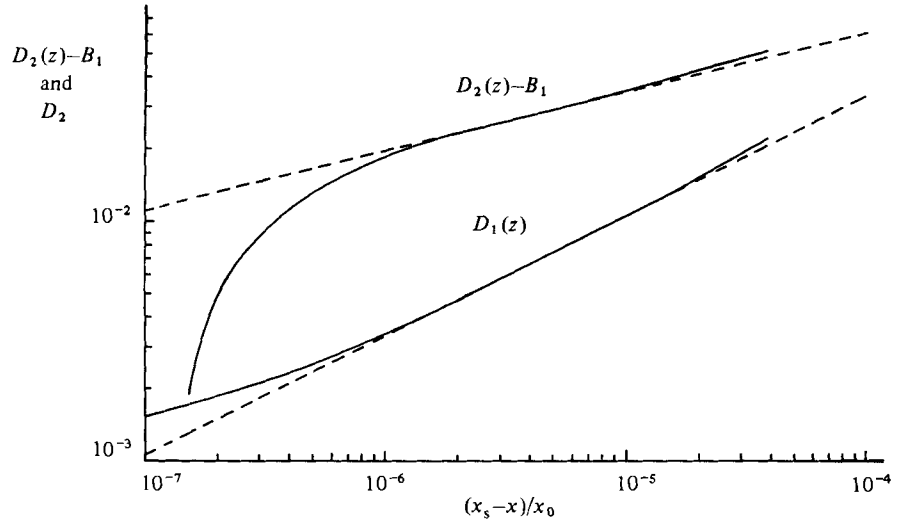


FIGURE 5. The distributions of $D_1(z)$ and $D_2(z)$ near separation for a cooled-wall case ($\lambda = 1.0$ and $S_w = -0.5$) with $Pr = 0.72$: ——, numerical results; – – –, Buckmaster's expansions with $\alpha_1 = 1.37$ and $B_1 = 0.180$.

(36). Expressing in terms of our transformed variables, we find from (34) and (39) that

$$Q_2(\xi) = -\frac{1+S_w}{S_w}\left[\frac{U_0[2\lambda+(1+S_w)(1-B_3^2(\xi))]}{2U_e(x_s)}\right]^{\frac{1}{2}} D_2(z). \tag{41}$$

With the two constants $\alpha_1$ and $B_1$ determined from the numerical results close to separation, the heat-transfer coefficient $Q_2(\xi)$ at the separation point $\xi_s$ can be calculated from (41). The computed results shown in table 4 are rather surprising; it seems to indicate that the heat-transfer coefficient at separation is constant for the

| $\lambda$ | $S_w$ | $\sigma_w \lambda^{-1}$ | $\alpha_1$ | $B_1$ | $Q_2$ at separation |
|---|---|---|---|---|---|
| 1.0 | 1.0 | $\frac{1}{2}$ | 1.40 | −0.102 | 0.208 |
| 1.0 | $-\frac{1}{2}$ | −1.0 | 1.37 | 0.180 | 0.184 |

TABLE 6. Values of $\alpha_1$, $B_1$ and $Q_2$ at separation; $Pr = 0.72$

class of compressible laminar boundary-layer flow governed by (1)–(8) with the external velocity described by (25) and (26) and the assumption of Prandtl number $Pr = 1.0$.

The effect of Prandtl number upon the solution close to separation has been investigated for a heated-wall case ($\lambda = 1.0$ and $S_w = 1.0$) and a cooled-wall case ($\lambda = 1.0$ and $S_w = -0.5$). For Prandtl number $Pr = 0.72$ and free-stream Mach number $M_\infty = 0.5$, the numerical results, presented in figures 4 and 5, clearly show that $D_1(z)$ is proportional to $(x_s - x)^{\frac{1}{2}}$ and that $D_2(z)$ is proportional to $(x_s - x)^{\frac{1}{4}}$. The results seem to indicate that Buckmaster's series solutions, (35) and (36), retain their validity for $Pr = 0.72$. The calculated constants $\alpha_1$ and $B_1$ and the heat transfer $Q_2$ at separation are given in table 6. Comparison with the entries of table 4 shows that the effect of Prandtl number on the heated-wall case is less than that on the cooled-wall case. Moreover, the computed heat-transfer coefficient at separation $Q_2(\xi_s)$ does vary with the wall temperature if the Prandtl number is not equal to unity.

## 6. Conclusions

Numerical solutions of the compressible laminar boundary-layer equations have been obtained for a number of flows that separate under the action of an adverse pressure gradient proportional to a positive parameter $\lambda$.

For $\lambda \geqslant 1.0$ the computed skin friction is in excellent agreement with Curle's asymptotic series solution obtained under the assumptions that $\lambda$ is large and $Pr = 1.0$. The computed heat-transfer distribution is in excellent agreement with Curle's results far from the separation point, but exhibits a steadily increasing difference as separation is approached. It is shown that Curle's series solutions cannot be used for $\lambda < 1.0$.

The nature of the singularity at the separation point has been investigated in detail. The numerical method employed allows the integration to be carried out to at least one integration step upstream of the separation point. The solutions for all cases run (nearly insulated, cooled and heated wall, $Pr = 1.0$) are in agreement with Buckmaster's series expansions derived for cold-wall separation. The two constants in Buckmaster's series expansions have been evaluated and the heat-transfer coefficient at the separation point determined. It is found that the heat-transfer coefficient at separation is relatively insensitive to wall-temperature conditions for $Pr = 1.0$.

A limited investigation of the flow characteristics for $Pr = 0.72$ seems to indicate that the nature of the singularity at separation remains unchanged.

## Appendix

The transformations used between (1)–(8) and (9)–(14) are summarized here. The motivation of each transformation and the detailed derivations of the transformed equations are given by Liakopoulos (1982).

The governing differential equations are written in terms of dimensionless variables by selecting as reference values the free-stream velocity $U_\infty$ and the characteristic length $L$ of the problem at hand. The new variables are

$$x_2 = \frac{x}{L}, \quad y_2 = \frac{y}{L}, \quad u_2(x_2, y_2) = \frac{u(x,y)}{U_\infty}, \quad v_2(x_2, y_2) = \frac{v(x,y)}{U_\infty},$$

$$S_2(x_2, y_2) = S(x, y).$$

A transformation is introduced so that the $x$-momentum and energy equations are independent of the Reynolds number, and the boundary conditions imposed on the variables related to $u_2$ and $S_2$ are the same for all boundary-layer flows of the class considered (Hsu 1976). The relations between the new and old variables are

$$x_3 = \int_0^{x_2} u_{2e}\, ds, \quad y_3 = Re^{\frac{1}{2}} u_{2e}(x_2)\, y_2,$$

$$u_3(x_3, y_3) = \frac{u_2(x_2, y_2)}{u_{2e}(x_2, y_2)}, \quad \theta_3(x_3, y_3) = \frac{1 - S_2(x_2, y_2)}{S_{2w}(x_2)},$$

$$v_2(x_2, y_2) = Re^{-\frac{1}{2}} u_{2e}\left[v_3(x_3, y_3) - y_3 u_3 \frac{d \ln u_{3e}}{dx_3}\right],$$

$$u_{3e}(x_3) = u_{2e}(x_2), \quad \Phi(x_3) = S_{2w}(x_2),$$

where

$$Re = U_\infty L/\nu_0.$$

The final transformation, which involves a distortion of $(x_3, y_3)$-coordinates and of the velocity and temperature functions, is defined by

$$\xi = \int_0^{x_3} \frac{ds}{s}, \quad \eta = x_3^{-\frac{1}{4}} \left(\int_0^{y_3} u_3(x_3, s)\, ds\right)^{\frac{1}{2}},$$

$$w(\xi, \eta) = u_3^2(x_3, y_3), \quad \phi(\xi, \eta) = \theta_3^2(x_3, y_3).$$

$$U(\xi) = u_{3e}(x_3), \quad \theta(\xi) = \Phi_3(x_3).$$

## REFERENCES


BUCKMASTER, J. 1970 The behaviour of a laminar compressible boundary layer on a cold wall near a point of zero skin friction. *J. Fluid Mech.* **44**, 237.

CURLE, N. B. 1958 The steady compressible laminar boundary layer, with arbitrary pressure gradient and uniform wall temperature. *Proc. R. Soc. Lond.* A **249**, 206.

CURLE, N. 1978 Development and separation of a compressible laminar boundary layer under the action of a very sharp adverse pressure gradient. *J. Fluid Mech.* **84**, 385.

DAVIES, T. & WALKER, G. 1977 On solutions of the compressible laminar boundary-layer equations and their behaviour near separation. *J. Fluid Mech.* **80**, 279.

GEAR, C. W. 1969 The automatic integration of stiff ordinary differential equations. In *Information Processing* (ed. A. J. H. Morrel), p. 187. North-Holland.

GOLDSTEIN, S. 1948 On laminar boundary layer flow near a position of separation. *Q. J. Mech. Appl. Maths* **1**, 43.

HSU, C. C. 1976 The use of splines for the solution of the boundary-layer equations. *Tech. Rep.* AFFDL-TR-75-158.

HSU, C. C. 1980 A finite element–differential method for a class of boundary-layer flows. In *Proc. 3rd Intl Conf. on Finite Elements in Flow Problems, Alberta, Canada.*

HSU, C. C. & CHANG, T. H. 1982 On a numerical solution of incompressible turbulent boundary layer flow. In *Finite Element Flow Analysis* (ed. T. Kawai), p. 219. University of Tokyo Press.

HSU, C. C. & LIAKOPOULOS, A. 1982 Nonsimilar solutions of compressible laminar boundary layer flows by a semi-discretization method. In *Finite Element Flow Analysis* (ed. T. Kawai), p. 395. University of Tokyo Press.

HUNT, R. & WILKS, G. 1980 On the behaviour of the laminar boundary-layer equations of mixed convection near a point of zero skin friction. *J. Fluid Mech.* **101**, 377.

KAPLUN, S. 1967 In *Fluid Mechanics and Singular Perturbations* (ed. P. A. Lagestrom, L. N. Howard & C. S. Liu). Academic.

LIAKOPOULOS, A. 1982 A finite element–differential method for compressible turbulent boundary-layer flows. Ph.D. dissertion, University of Florida.

LIAKOPOULOS, A. 1984 Computation of high speed turbulent boundary-layer flows using the $k$-$\epsilon$ turbulence model. *Intl J. Numer. Meth. Fluids* (to appear).

MERKIN, J. H. 1969 The effect of buoyancy forces on the boundary-layer flow over a semi-infinite vertical flat plate in a uniform free stream. *J. Fluid Mech.* **35**, 439.

POOTS, G. 1960 A solution of the compressible laminar boundary layer equation with heat transfer and adverse pressure gradient. *Q. J. Mech. Appl. Maths* **13**, 57.

STEWARTSON, K. 1958 On Goldstein's theory of laminar separation. *Q. J. Mech. Appl. Maths* **13**, 57.

STEWARTSON, K. 1962 The behaviour of a laminar compressible boundary layer near a point of zero skin-friction. *J. Fluid Mech.* **12**, 117.

WERLE, M. J. & SENECHAL, G. D. 1973 A numerical study of separating supersonic laminar boundary layers. *Trans. ASME* E: *J. Appl. Mech.* **40**, 679.